Journal of Theoretical and Applied Physics (JTAP), Special Issue: AICIS'23-Article 20

Proceeding of the 3rd Annual International Conference on Information and Sciences 2023, University of Fallujah, Iraq

https://dx.doi.org/10.57647/j.jtap.2024.si-AICIS23.20

Modifying ZnO nanopowders with ZrO_2 prepared by atmospheric pressure plasma jet synthesis and continuous laser diode treatment

Ahmed Abed Anber[1,*], Ammar S. Hameed[2], Mohammed Oudah Salman[3]

[1]*Department of Renewable Energy Science, College of Energy and Environment Science, AL-Karkh University of Science, Baghdad, Iraq.*
[2]*Department of Physics, College of Science, University of Kerbala, Karbala, Iraq.*
[3]*Department of Medical Physics, College of Applied Science, University of Fallujah, Iraq.*

[*]**Corresponding author:** Ahmed.abed@kus.edu.iq

Original Research

Published online: 15 June 2024

Abstract:

In this work, zinc oxide nanopowders (ZnO-NPs) were synthesized by atmospheric pressure plasma jet and continuous laser diode (CLD) techniques. ZrO_2 powder were made up with the ZnO nanopowders to study its effect on ZnO properties. The study initiated with the utilization of the atmospheric pressure plasma jet technique recognized for its capability to generate nanoparticles using cold plasma, ensuring high purity and controlled growth. Following this, CLD techniques were employed to fine-tune the structural attributes of the ZnO-ZrO_2 nanocomposite. The average particle size and morphology were examined by FE-SEM, and the crystallinity was estimated by XRD analysis and the spectroscopic properties of the powder were measured by using FTIR spectroscopy. XRD studies confirm that zinc oxide has a high degree of crystallinity. The particle size of ZnO was found to be about 18 nm. The purpose of this study involved the investigation of ZnO nanoparticle characteristics. The outcome considered a new synthesis of ZnO nanopowders that may be employed in many scientific applications using continuous laser diode to increase the oxidization. This is represented as a novel method and also a simple and cost effective one.

Keywords: ZnO nanopowders; Atmospheric pressure plasma jet; Continuous laser diode, FTIR spectroscopy

1. Introduction

Nanotechnology, with its ability to manipulate matter at the atomic and molecular scale, continues to develop materials science, offering new roads for advanced materials with different properties [1]. Zinc oxide (ZnO) nanoparticles have emerged as a focal point in nanomaterial research due to their unique properties and adaptable applications across various scientific fields [2]. The synthesis and modification of ZnO nanoparticles offer opportunities for unprecedented advancements in material science and technology [3]. Pure ZnO nanoparticles have notable intrinsic semiconductor characteristics, exceptional transparency, and remarkable photostability [4]. These properties make them invaluable in numerous applications, covering optoelectronics, catalysis, sensing, and biomedical fields [5]. The ability to harness ultraviolet (UV) light and exhibit photocatalytic activity positions pure ZnO nanoparticles as promising candidates for solar energy harvesting [6], environmental cleaning, and antibacterial applications [7].

Doping ZnO nanoparticles with various elements introduces a tailored approach to fine-tune their properties [8]. This incorporation of dopants such as metal ions, transition metals, or other semiconductors offers control over electronic, optical, and structural attributes, expanding the range of potential applications [9]. Among the diverse dopants, emphasis is often placed on elements like aluminum (Al), gallium (Ga), and zirconia (ZrO_2), each imparting unique functionalities to the ZnO matrix [10]. Synthesizing ZnO nanoparticles demands precision, and various techniques have been developed to control size, shape, and composition [11]. Traditional methods include sol-gel, hydrothermal, and pre-

cipitation methods, while more recent approaches employ advanced techniques such as microwave-assisted synthesis and atmospheric pressure plasma jet [12]. Therefore, the preparation method always determines the final properties of the nanoparticles [13].

In nanomaterials, the incorporation of zirconia (ZrO_2) into zinc oxide (ZnO) nanoparticles is a powerful strategy for engineering enhanced functionalities and expanding the scope of applications [14]. Zirconia, characterized by its high thermal stability and mechanical properties, imparts unique characteristics to ZnO nanoparticles when intentionally introduced as a dopant. This intentional addition serves as a precision engineering approach to tailor the structural, morphological, and optical properties of ZnO, offering unique control over the material's behavior [15].

The semiconducting nature and excellent optical properties of ZnO nanoparticles, both pure and doped, make them candidates for the development of high-performance optoelectronic devices [16]. Also, engineered ZnO nanoparticles find application in gas sensors, biosensors, and environmental monitoring devices. Surface-modified ZnO nanoparticles, often doped for specific functionalities, exhibit biocompatibility and can be employed in drug delivery systems, imaging agents, and cancer therapy [17]. ZnO nanoparticles, when doped with suitable materials, become efficient catalysts for a range of chemical reactions, providing opportunities for sustainable and environmentally friendly processes [18]. Also, the incorporation of ZrO2 can enhance the mechanical properties and thermal stability of ZnO [19].

This study explores the integration of zirconia (ZrO_2) additives into zinc oxide (ZnO) nanopowders, synthesized through atmospheric pressure plasma jet techniques and subsequently refined using continuous laser diode treatments. The investigation aims to unravel the nuanced impact of ZrO_2 on the structural, morphological, and optical properties of the resulting anocomposites, with a particular focus on elucidating potential applications in diverse technological domains. The results are expected to advance our understanding of anocomposites design and foster innovative applications across multiple disciplines.

2. Experimental setup

zinc oxide nanopowders were synthesized through an atmospheric plasma jet system. The cathode, constructed from stainless steel with an inner diameter of 0.5 mm and a length of 8 cm, was positioned 2 cm away from the anode (zinc sheet). The anode, measuring 5 cm in width, 10 cm in length, and with a 2 cm^2 immersion area, was securely fixed with a 2 mm gap between the tube end and the liquid surface. Argon gas, flowing through the tube at a rate of 65 mL/min and regulated by a glass flow meter, served as the discharge gas. The chemical reaction took place in a glass beaker, with the polished Zn anode immersed in an electrolyte containing 1 g/L NaOH, 1.3 g/L HNO_3, and 1 g/L glucose (fructose) as stabilizers to prevent uncontrolled particle growth and agglomeration. The discharge initiation involved applying a high voltage of 3 kV with a frequency of 40 KHz using an AC power supply while maintaining a constant discharge current within the range of 5 – 10 mA. The electrolyte exposure varied in duration (15, 30, and 45 minutes), and the resulting sediments underwent centrifugation, washing with deionized water and ethanol, and drying at 60 °C for 2 hours. Subsequently, ZrO_2 was added in different proportions (10% ZrO_2 + 90% ZnO, 20% ZrO_2 + 80% ZnO, and 50% ZrO_2 + 50% ZnO). The compositions underwent annealing using a continuous laser diode system with a laser power of 1500 mW and a wavelength of 405 nm, controlled by software. This diode laser was used to improve the oxidization of the prepared nanoparticles. The prepared nanoparticles were studied by X-ray diffraction, FE-SEM, and FTIR spectroscopy to explore changes in crystalline structure, morphology, and molecular structure by introducing the ZrO_2 into the system of the prepared nanoparticles. Fig. 1 shows the experimental setup.

3. Results and discussion

Fig. 2 shows the X-ray diffraction analysis of the ZnO-ZrO_2 nanocomposite within the range of 10° to 80°. The diffraction patterns displayed numerous diffraction peaks consistent with the JCPDS card 96-901-1663. The three noticeable diffraction lines located at Bragg's angles (2θ) correspond to Miller indices (hkl) of 31.88° (100), 34.49° (002), and 36.5125° (101), corresponding to hexagonal ZnO crystal. Concurrently, minor diffraction peaks emerged, corresponding to the cubic shape of ZrO_2 crystallites in the JCPDS card 96-152-2144. These peaks intensified with increasing ZrO_2 content. The positional, intensity, and broadening characteristics of these peaks provided insights into the strain, composition, and crystallite size of the ZnO-

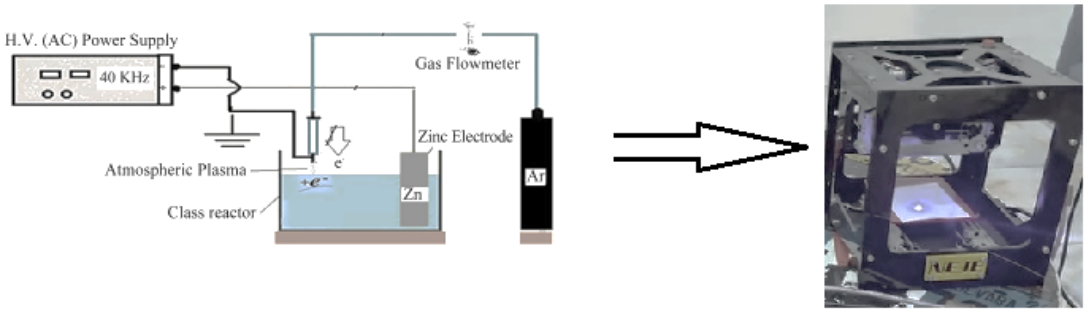

Figure 1. Experimental setup.

ZrO_2 particles. Utilizing the Scherrer formula, the average crystallite size for ZnO nanocrystallites was determined to be 16.2 nm, while for ZrO_2 crystals, it was 12.5 nm. Interestingly, ZrO_2 crystallites exhibited a smaller size than ZnO nanocrystallites, possibly attributable to their lower concentration. The narrower Bragg's diffraction lines suggested the highly crystalline nature of ZnO nanocrystallites relative to ZrO_2. Additionally, the presence of noisy diffraction spectra hinted at the existence of some amorphous content in the sample. Notably, a negative shift in the 2θ value was observed, possibly indicating the introduction of strain in the ZnO crystallite lattice due to the intrusion of zirconium cations substituting into the lattice.

Fig. 3 depicts the compositional morphology, as analyzed through field emission scanning electron microscopy (FE-SEM). The structure exhibits irregular formations around 50 nm diameter interconnected to constitute the overall entity. The impact of introducing ZrO_2 to ZnO powders is evident. Notably, at a ZrO_2-ZnO ratio of 10% ZrO_2 + 90% ZnO, the surface displays small white particles attached to the surface and structural vacancies, as illustrated in Fig. 2(a). As the ZrO_2 ratio increases from 20% to 50%, the accumulation dots increase while the vacancies diminish, as observed in Figs. 2(b, c). This additive has the potential to augment the hardness of ZnO nanostructures by mitigating the presence of vacancies. The emergence of two-particle modes aligns with the result of two distinct phases, as exposed in the XRD test.

In the context of ZnO-ZrO_2 nanoparticles prepared via plasma jet, FTIR analysis was employed to elucidate the compositional bond configurations within the 400 to 4000 cm^{-1} spectral range. In the initial configuration (10% ZrO_2 + 90% ZnO), a strong and broad absorption band at approximately 532.84 cm^{-1} was identified, corresponding to the Zn-O bond. Broad absorption bands were also evident at 3446.49 and 1635.42 cm^{-1}, indicative of O-H stretching and bending modes, respectively. Upon transitioning to a 20% ZrO_2 ratio, distinctive absorption bands at 749.82 cm^{-1} and 763.10 cm^{-1} emerged, attributed to the Zr-O bond. These bands intensified with a further increase in the ZrO_2 ratio to 50%. Simultaneously, Zn-O absorption bands at 546.13 cm^{-1} (80% ZrO_2) and 537.27 cm^{-1} (50% ZrO_2)

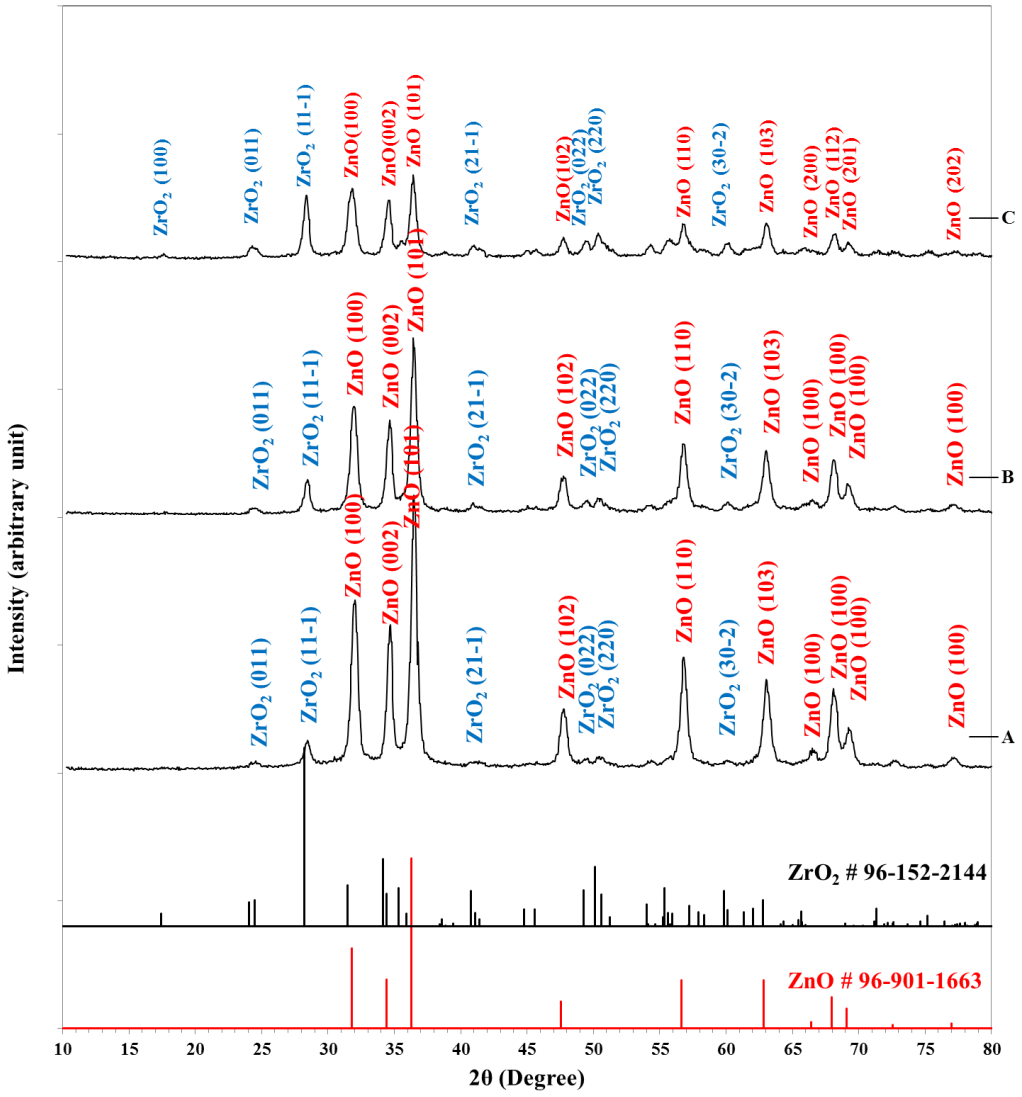

Figure 2. The XRD patterns of ZnO: ZrO_2 nanopowder at different ratios.

displayed a reduction in intensity. Notably, an additional band around 1369 cm^{-1} surfaced, indicative of an intermediate phase of metal hydroxide. These FTIR findings provide detailed insights into the evolving bond configurations within the ZnO-ZrO_2 composite nanoparticle under varying ratios.

4. Conclusion

In conclusion, this study contributes to the evolving landscape of nanomaterials by exploring the effects of ZrO_2 additives in ZnO nanopowders. The outcomes of this study hold promise for diverse applications, including advanced photocatalysis for environmental remediation, optoelectronic devices such as sensors and solar cells, and biomedical applications. The tailored properties of the ZnO-ZrO_2 nanocomposite are poised to unlock new possibilities in materials engineering and technology development.

Authors Contributions
Authors have contributed equally in preparing and

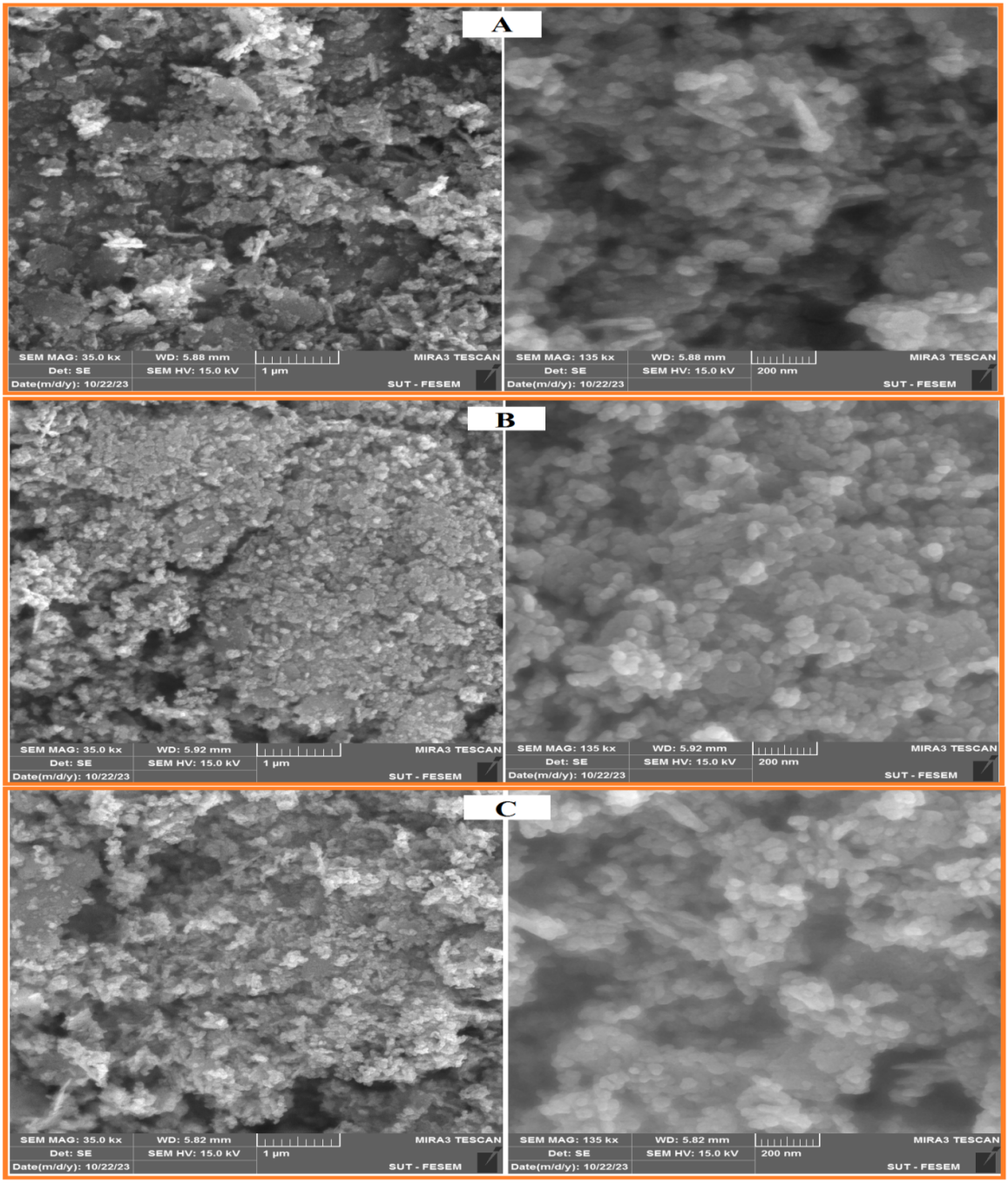

Figure 3. FE-SEM image measurements of the fabricated ZnO-ZrO_2 nano composited A) 10% ZrO_2 + 90% ZnO, B) 20% ZrO_2 + 80% ZnO and, C) 50% ZrO_2 + 50% ZnO.

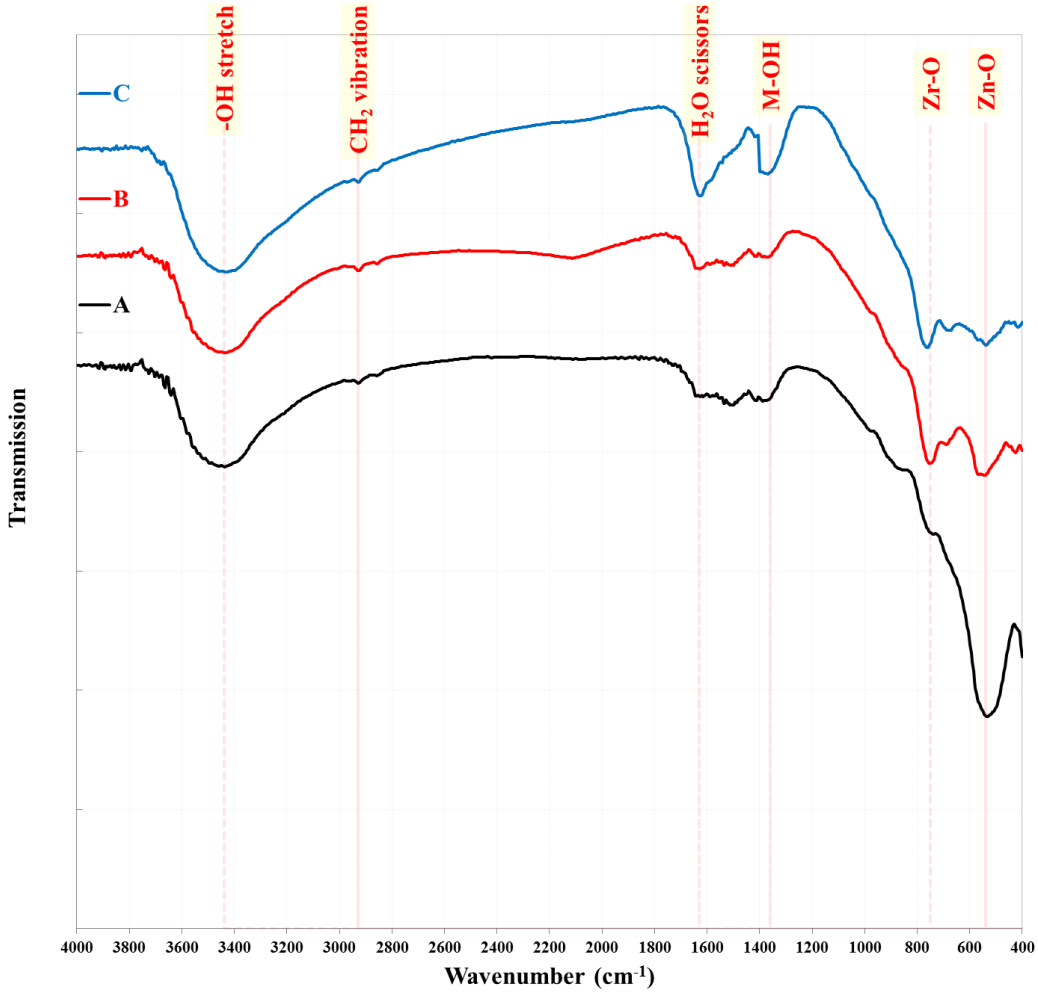

Figure 4. FTIR spectrum of ZnO with different ZrO_2 A) 10% ZrO_2 + 90% ZnO ,B) 20% ZrO_2 + 80% ZnO and, C) 50% ZrO_2 + 50% ZnO.

Table 1. XRD parameter of ZnO with different ZrO_2 concentration.

Sample	2θ (Deg.)	FWHM (Deg.)	d_{hkl} Exp.($\AA$)	C.S (nm)	Aver. C.S (nm)	hkl	Phase
A	28.4187	0.6563	3.1381	12.5	12.5	(11-1)	Cubic. ZrO_2
	32.0500	0.6125	2.7904	13.5	16.2	(100)	Hex. ZnO
	34.6750	0.4375	2.5849	19.0		(002)	Hex. ZnO
	36.5125	0.5251	2.4589	15.9		(101)	Hex. ZnO
B	28.4625	0.5450	3.1334	15.0	15.0	(11-1)	Cubic. ZrO_2
	32.0063	0.6562	2.7941	12.6	14.4	(100)	Hex. ZnO
	34.6312	0.5250	2.5881	15.9		(002)	Hex. ZnO
	36.4688	0.5688	2.4618	14.7		(101)	Hex. ZnO
C	28.3750	0.5288	3.1429	15.5	15.5	(11-1)	Cubic. ZrO_2
	31.9187	0.8313	2.8015	9.9	12.7	(100)	Hex. ZnO
	34.5438	0.5687	2.5944	14.6		(002)	Hex. ZnO
	36.4688	0.6126	2.4618	13.7		(101)	Hex. ZnO

Table 2. Bonds in FTIR spectra of ZnO with different ZrO_2 concentration.

Band Type	A	B	C
O-H stretch	3446.49	3433.21	3446.49
CH_2	2923.99	2923.99	2923.99
H_2O	1635.42	1626.57	1626.57
M-OH	1369.74	1365.31	1365.31
Zr-O	——	749.82	763.10
Zn-O	532.84	546.13	537.27

writing the manuscript.

Availability of data and materials
Data presented in the manuscript are available via request.

Conflict of Interests
The author declare that they have no known competing financial interests or personal relationships that could have appeared to influence the work reported in this paper.

References

[1] S. Malik, K. Muhammad, and Y. Waheed. "Nanotechnology: a revolution in modern industry.". *Molecules*, **28**:661, 2023.

[2] X.-Q. Zhou, Z. Hayat, D.-D. Zhang, M.-Y. Li, S. Hu, Q. Wu, Y.-F. Cao, and Y. Yuan. "Zinc oxide nanoparticles: synthesis, characterization, modification, and applications in food and agriculture.". *Processes*, **11**: 1193, 2023.

[3] I. Khana, K. Saeed, and I. Khan. "Nanoparticles: properties, applications and toxicities.". *Arab. J. Chem.*, **12**:908–931, 2019.

[4] S. Arya, P. Mahajan, S. Mahajan, A. Khosla, R. Datt, V. Gupta, S.-J. Young, and S. K. Oruganti. "Review—influence of processing parameters to control morphology and optical properties of sol-gel synthesized ZnO nanoparticles.". *ECS J. Solid State Sci. Technol.*, **10**:023002, 2021.

[5] S. Raha and M. Ahmaruzzaman. "ZnO nanostructured materials and their potential applications: progress, challenges and perspectives.". *Nanoscale Adv.*, **4**: 1868–1925, 2022.

[6] B. Bagchi, N. A. Hoque, N. Janowicz, S. Das, and M. K. Tiwari. "Re-usable self-poled piezoelectric/piezocatalytic films with exceptional energy harvesting and water remediation capability.". *Nano Energy.*, **78**:105339, 2020.

[7] J. Theerthagiri, S. Salla, R. A. Senthil, P. Nithyadharseni, A. Madankumar, P. Arunachalam, T. Maiyalagan, and H.-S. Kim. "A review on ZnO nanostructured materials: energy, environmental and biological applications.". *Nanotechnology*, **30**:392001, 2019.

[8] P. Kumari, K. P. Misra, S. Chattopadhyay, and S. Samanta. "A brief review on transition metal ion doped ZnO nanoparticles and its optoelectronic applications. ". *Mater. Today Proc.*, **43**:3297–3302, 2021.

[9] S. G. Kumar, R. Kavitha, and C. Sushma. "Doped zinc oxide nanomaterials: structure–electronic properties and photocatalytic applications, in: 2020: pp. 285–312 ". *Interface Science and Technology*, **31**: 285–312, 2020.

[10] U. B. Isyaku, M. H. B. M. Khir, I. M. Nawi, M. A. Zakariya, and F. Zahoor. "ZnO based resistive random access memory device: a prospective multifunctional next-generation memory.". *IEEE Access.*, **9**: 105012–105047, 2021.

[11] M. Sajid and J. Płotka-Wasylka. "Nanoparticles: Synthesis, characteristics, and applications in analytical and other sciences". *Microchem. J.*, **154**:104623, 2020.

[12] Q. Zhang, J. Li, and M. Xu. "Ag-decorated ZnO-based nanocomposites for visible light-driven photocatalytic degradation: basic understanding and outlook. ". *J. Phys. D. Appl. Phys.*, **55**:483001, 2022.

[13] F. Islam, S. Shohag, M. J. Uddin, M. R. Islam, M. H. Nafady, A. Akter, S. Mitra, A. Roy, T. Bin Emran, and S. Cavalu. "Exploring the Journey of zinc oxide nanoparticles (ZnO-NPs) toward biomedical applications. ". *Materials (Basel)*, **15**:2160, 2022.

[14] J. A. Kumar, T. Krithiga, S. Manigandan, S. Sathish, A. A. Renita, P. Prakash, B. S. N. Prasad, T. R. P. Kumar, M. Rajasimman, A. Hosseini-Bandegharaei,

D. Prabu, and S. Crispin. "A focus to green synthesis of metal/metal based oxide nanoparticles: Various mechanisms and applications towards ecological approach.". *J. Clean. Prod.*, **324**:129198, 2021.

[15] P. K. Haldar, T. K. Parya, and S. Mukhopadhyay. "Effect of Zr^{4+} dopant on microstructure, densification and thermomechanical behaviour of $ZnAl_2O_4$ spinel. ". *Interceram - Int. Ceram. Rev.*, **69**:44–49, 2020.

[16] V. Doni Pon, K. S. Joseph Wilson, K. Hariprasad, V. Ganesh, H. Elhosiny Ali, H. Algarni, and I. S. Yahia. "Enhancement of optoelectronic properties of ZnO thin films by Al doping for photodetector applications.". *Superlattices Microstruct*, **151**:106790, 2021.

[17] V. J. Raj, R. Ghosh, A. Girigoswami, and K. Girigoswami. "Application of zinc oxide nanoflowers in environmental and biomedical science.". *BBA Adv.*, **2**:100051, 2022.

[18] K. V. Karthik, A. V. Raghu, K. R. Reddy, R. Ravishankar, M. Sangeeta, N. P. Shetti, and C. V. Reddy. "Green synthesis of Cu-doped ZnO nanoparticles and its application for the photocatalytic degradation of hazardous organic pollutants. ". *Chemosphere.*, **287**, 2022.

[19] H. Majidian, M. Farvizi, and L. Nikzad. "Introducing MnO_2 and ZnO additives for the development of alumina–mullite–zirconia composites. ". *JOM.*, **73**: 3486–3496, 2021.